Electronic Supplementary Material (ESI) for Molecular BioSystems.

Supporting Information

Enantioselective recognition of isomeric ligand by biomolecule: Mechanistic insights from static, dynamic enantiomeric behavior and structural flexibility

Wei Peng,[abc] and Fei Ding*[a]

[a] *Laboratory for Computational Biochemistry & Molecular Design, Department of Phytomedicine, Qingdao Agricultural University, Qingdao 266109, China*

[b] *School of Pharmaceutical Science and Technology, Tianjin University, Tianjin 300072, China*

[c] *Department of Chemistry, China Agricultural University, Beijing 100193, China*

*Corresponding Author
Phone/fax: +86-29-87092367
E-mail: alexf.ting@outlook.com

Supplementary Experimental:

Materials. Albumin from human serum (A3782, lyophilized powder, fatty acid free, globulin free, ≥99%, CAS number 70024-90-7), diazepam (D0899, CAS number 439-14-5), diclofop (52256, ≥98%, CAS number 40843-25-2), digitoxin (D5878, ≥92%, CAS number 71-63-6), hemin (H9039, ≥90%, CAS number 16009-13-5) and warfarin (A2250, CAS number 81-81-2) were purchased from Sigma-Aldrich (St. Louis, MO) and used without further purification, and deionized water was generated by a Milli-Q Ultrapure Water Purification Systems from Millipore (Billerica, MA). Tris (0.2 M)-HCl (0.1 M) buffer of pH＝7.4, with an ionic strength 0.1 in the presence of NaCl, and the pH was checked with an Orion Star A211 pH Benchtop Meter (Thermo Scientific, Waltham, MA). Dilutions of the protein stock solution (10 μM) in Tris-HCl buffer were prepared immediately before use, and the concentration of protein was measured by the method of Lowry et al.[1] All other reagents employed were of analytical grade and received from Sigma-Aldrich. To remove any undissolved matter, all samples were filtered through a 0.22 μm Millex-GV Filter (Millipore, Billerica, MA).

Steady-State Fluorescence. Steady-state fluorescence was obtained with a 1.0 cm path length quartz cell using a F-7000 spectrofluorimeter (Hitachi, Japan) equipped with a thermostatic bath. The excitation and emission slits were set at 5.0 nm each, intrinsic fluorescence was carried out by exciting the continuously stirred protein solution at 295 nm to favor tryptophan (Trp) excitation, and the emission spectra were read in the wavelength range of 300～450 nm at a scanning speed of 240 nm min^{-1}. The reference sample consisting of the Tris-HCl buffer of diclofop enantiomers in corresponding concentrations was subtracted from all fluorescence measurements.

Time-Resolved Fluorescence. Time-resolved fluorescence was examined with a FLS920 spectrometer (Edinburgh Instruments, UK), using the time-correlated single photon counting system with a hydrogen flash lamp excitation source, in air equilibrated solution at an ambient temperature. The excitation wavelength was 295 nm and the number of counts gathered in the channel of maximum intensity was 4,000. The instrument response function (IRF) was gauged exploiting Ludox to scatter light at the excitation wavelength. The data were analyzed with a nonlinear least-squares iterative method utilizing the Fluorescence Analysis Software Technology, which is a sophisticated software package designed by Edinburgh Photonics for the analysis of fluorescence and phosphorescence decay kinetics, IRF was deconvoluted from the experimental data, and the resolution limit after deconvolution was 0.2 ns. The value of χ^2 (0.9～1.2), the Durbin-Watson parameter (greater than 1.7), as well as a visual inspection of the residuals were used to assess

how well the calculated decay fit the data. Average fluorescence lifetime (τ) for multiexponential function fittings were from the following relation:[2]

$$I(t) = \sum_i A_i e^{\frac{-t}{\tau_i}} \quad (1)$$

where τ_i are fluorescence lifetimes and A_i are their relative amplitudes, with i variable from 1 to 2.

Site-Specific Competitive Experiments. Biorecognition patch studies between protein and diclofop enantiomers in the presence of four classic site markers (warfarin, diazepam, digitoxin and hemin) were executed using the fluorescence titration approach. The concentration of protein and site markers were held in equimolar (1.0 μM), then diclofop enantiomers were respectively added to the protein-site markers mixtures. An excitation wavelength of 295 nm was chosen and the fluorescence emission wavelength was acquired from 300 to 450 nm.

Extrinsic ANS Displacement. In the first series of experiments, protein concentration was kept fixed at 1.0 μM, and diclofop enantiomers/ANS concentration was varied from 2.0 to 18 μM, protein fluorescence was gained (λ_{ex}＝295 nm, λ_{em}＝333 nm). In the second series of experiments, diclofop enantiomers were respectively added to solutions of protein and ANS held in equimolar concentration (1.0 μM), and the concentration of diclofop enantiomers was also varied from 2.0 to 18 μM, the fluorescence of ANS was recorded (λ_{ex}＝370 nm, λ_{em}＝465 nm).

Circular Dichroism. Circular dichroism (CD) were collected with a Jasco-815 spectropolarimeter (Jasco, Japan) equipped with a microcomputer, the apparatus was sufficiently purged with 99.9% dry nitrogen gas before starting the instrument and then it was calibrate with d-10-camphorsulfonic acid. All the CD spectra were got at 298 K with a PFD-425S Peltier temperature controller attached to a water bath with an accuracy of ±0.1 ^{o}C. Each spectrum was performed with use of a precision quartz cuvette of 1.0 cm path length and taken at wavelengths between 200 and 260 nm range that provides a signal extremely sensitive to small secondary conformational distortions. Every determination was the average of five successive scans encoded with 0.1 nm step resolution and recorded at a speed of 50 nm min^{-1} and response time of 1 s. All observed CD data were baseline subtracted for buffer and the estimation of the secondary structure elements was obtained by exploiting Jasco Spectra Manager II, which computes the different designations of secondary structures by comparison with CD spectra, determined from distinct proteins for which high-quality X-ray diffraction data are available.

Ligand Docking. *In silico* docking of the protein-diclofop enantiomers was operated on SGI Fuel Visual Workstation. The crystal structure of protein (entry codes 1AO6),[3] determined at a resolution 2.5 Å, was retrieved from the Brookhaven

Protein Data Bank (http://www.rcsb.org/pdb). After being imported in the program SYBYL Version 7.3 (http://www.certara.com), protein structure was carefully checked for atom and bond type correctness assignment. Hydrogen atoms were computationally added using the SYBYL Biopolymer and Build/Edit menus. To avoid negative acid/acid interactions and repulsive steric clashes, added hydrogen atoms were energy minimized with the Powell algorithm with 0.05 kcal mol^{-1} energy gradient convergence criteria for 1500 cycles,[4] this procedure does not change positions to heavy atoms, and the potential of the three-dimensional structure of protein was assigned according to the AMBER force field with Kollman all-atom charges.[5] The two-dimensional structures of diclofop isomers were downloaded from PubChem (https://pubchem.ncbi.nlm.nih.gov), and the initial structures of the stereoisomers were produced by SYBYL 7.3. The geometries of diclofop enantiomers were subsequently optimized to minimal energy (tolerance of 0.5 kcal mol^{-1}) using the Tripos force field with Gasteiger-Hückel charges,[6] and the lowest energy conformer was utilized for the docking analysis. The Surflex-Dock program which employs an automatic flexible docking algorithm was applied to analyze the possible conformations of the optical isomers that bind to protein, and the program PyMOL (http://www.schrodinger.com) was finally used for visualization of the molecular docking results.

Calculation of Free Energies. Binding free energies of the protein-diclofop enantiomers were computed by using the Amber Molecular Dynamics Package (University of California, San Francisco, CA) based upon the approach of Molecular Mechanics/Generalized Born Surface Area (MM/GBSA), and the relevant relationships for the MM/GBSA enumerations are given by[7]

$$\Delta G_{bind} = G_{complex} - (G_{protein} + G_{ligand}) \tag{2}$$

$$E_{MM} = E_{vdW} + E_{ele} \tag{3}$$

$$G = \langle E_{MM} \rangle + \langle G_{nonpol,sol} \rangle + \langle G_{pol,sol} \rangle - T \langle S \rangle \tag{4}$$

$$G_{nonpol,sol} = \gamma \times SASA + b \tag{5}$$

In these equations the binding free energy, ΔG_{bind}, is constituted of the classical $E_{products} - E_{reactants}$ (the endpoints), where $E_{products} = \Delta G_{complex}$ and $E_{reactants}$ is composed of $G_{protein}$ and G_{ligand}. The molecular mechanics energy (E_{MM}) is made up of the van der Waals energy (including the internal energy) (E_{vdW}) and the electrostatic energy (E_{ele}). The polar solvation ingredient ($G_{pol,sol}$) is estimated utilizing the generalized Born method. The nonpolar solvation element ($G_{nonpol,sol}$) is reckoned using solvent accessible area with the γ parameter set to 0.00542 kcal (mol $Å^2$)$^{-1}$, and the b

parameter set to 0.92 kcal mol^{-1}. The Solvent Accessible Surface Area (SASA) is measured employing the linear combination of pairwise overlaps (LCPO) model.[8]

Principles of Fluorescence Spectroscopy. The intensity of fluorescence can be lessened by a vast variety of processes and such declines in intensity are intituled quenching. Fluorescence quenching could occur by different mechanisms. Collisional reaction occurs when the excited-state fluorophore is deactivated upon contact with quencher/ligand enantiomers in aqueous solution. In this case the fluorophore is returned to the ground-state during a diffusive encounter with the quencher/ligand enantiomers. The molecules are not chemically altered in the process. For collisional reaction the reduction in fluorescence intensity is portrayed by the well-known Stern-Volmer relation:[2,9]

$$\frac{F_0}{F} = 1 + k_q \tau_0 [Q] = 1 + K_{SV}[Q] \tag{6}$$

In this equation F_0 and F are the fluorescence intensities in the absence and presence of quencher/ligand enantiomers, respectively; k_q is the bimolecular reaction constant; τ_0 is the unquenched lifetime of the fluorophore; K_{SV} is the Stern-Volmer reaction constant, and $[Q]$ is the quencher/ligand enantiomers concentration. Aside from collisional reaction, fluorescence quenching might occur by a variety of other processes. Fluorophores may form nonfluorescent adducts with quenchers/ligand enantiomers. This process is referred to as static reaction since it occurs in the ground-state and does not rely on diffusion or molecular collisions. Fluorescence quenching can also occur by a variety of trivial, i.e. non-molecular mechanisms, e.g. attenuation of the incident light by the fluorophore itself or other absorbing species.

Estimation of Chiral Bioreaction Strength. When ligand enantiomers bind individually to a set of equivalent sites on a biomacromolecule, the equilibrium between free and bound ligand enantiomers is given by the following equation:[10,11]

$$\log \frac{F_0 - F}{F} = \log K + n \log[Q] \tag{7}$$

In this relationship, F_0 and F are the fluorescence intensities in the absence and presence of ligand enantiomers, respectively; K and n are the chiral bioreaction strength and the stoichiometry, respectively, and $[Q]$ is the concentration of ligand enantiomers. Thus, a plot of $\log(F_0 - F)/F$ *against* $\log[Q]$ can be used to calculate K and n. The fluorescence intensities were corrected for absorption of the exciting light and reabsorption of the emitted light to diminish the inner filter effect by using the following relationship:[12,13]

$$F_{cor} = F_{obs} \times e^{\frac{A_{ex} + A_{em}}{2}} \tag{8}$$

where F_{cor} and F_{obs} are the fluorescence intensities corrected and observed, respectively, and A_{ex} and A_{em} are the absorption of the systems at the excitation and

147 the emission wavelength, respectively. The fluorescence intensity utilized in this
148 study is the corrected intensity.

Supplementary Results and Discussion:

Mechanism of Stereoselective Biorecognition. According to the results of fluorescence assays, one can observe that the differences of the enantioselective biointeraction are preserved between the functional biomacromolecule and the chiral active diclofop under simulated physiological conditions. To further comprehend such enantiomeric interactions, it is necessary to hunt the bioreaction mechanism of the chiral recognition. As mentioned earlier, the decrease of fluorescence intensity (quenching) has extensively been investigated both as a basic phenomenon, and as an origin of information about biochemical systems. These biological applications of fluorescence quenching are owing to the molecular interactions that result in quenching. Usually both static and dynamic reaction requests molecular contact between the fluorophore (Trp residue) and quencher (diclofop enantiomers). Upon contact, the fluorophore returns to the ground-state without emission of a photon. This means quenching occurs without any permanent change in the molecules, i.e. without a photochemical reaction.[14,15] We could consider that the determinations of quenching may be used to disclose the localization of fluorophores in proteins and their permeabilities to quenchers/ligand enantiomers, and the rate of collisional reaction might also be used to measure the diffusion coefficient of the quenchers/ligand enantiomers. Thereby the emergence of quenching rests on the chemical properties of the independent molecules, and detailed analysis of the mechanism of fluorescence quenching can help to realize the secret heart of chiral biorecognition.

The classic Stern-Volmer equation (6) was used for dealing with the data of steady-state fluorescence, and the corresponding outcomes fitted from Stern-Volmer plots Fig. S1 were summarized in Table S1. A plot of F_0/F *versus* [*Diclofop Enantiomers*] yields an intercept of one on the *y*-axis and a slope equal to K_{SV}. Intuitively, a linear Stern-Volmer plot is generally indicative of a single class of fluorophores, all equally accessible to quencher. Under the circumstances the protein holds a fluorophore – aromatic Trp-214 residue, which could be bioreacted perfectly with (*R*)-/(*S*)-diclofop. Meanwhile, the Stern-Volmer plot is linear, which also indicates that only one type of quenching occurs. However, it is important to recognize that observation of a linear Stern-Volmer plot does not prove that collisional reaction of fluorescence has happened. Static reaction also results in linear Stern-Volmer plots. Prosperously, the Stern-Volmer reaction constant K_{SV} is clearly reduced with the temperature elevation, and this is a compelling ammunition of the formation of the noncovalent adducts between the protein and chiral compound, as higher temperatures will typically result in the dissociation of weakly bound complexes, and hence smaller amounts of static reaction.[16,17] Furthermore, the order

of magnitude of the bimolecular reaction constant k_q at different temperatures is 10^{12}, which proposes efficient quenching by diclofop enantiomers via static type, since a bimolecular reaction constant near 1.0×10^{10} M^{-1} s^{-1} may be considered as the largest possible value for the diffusion-controlled reaction in aqueous solution. Accordingly, we might reasonably submit that decrease of protein fluorescence by two diclofop stereoisomers is purely static in this case, or rather, the stereoselective biointeraction of (*R*)-/(*S*)-diclofop with biomacromolecule is proceeded primarily through the appearance of the fluorophore-chiral ligand bioconjugates. This essay would attentively discuss the influence of chiral chemical on the chromophore by means of time-resolved fluorescence technique in the following content, in order to comprehensively illustrate the mode of action of the enantioselective bioreaction.

Commonly, the measurement of fluorescence lifetimes is the most definitive approach to discriminate static and dynamic reaction, and the main reason is that static reaction eliminates a fraction of the fluorophores from detection. The bound fluorophores are nonfluorescent, and the only observed fluorescence is from the unbound fluorophores. The unbound fraction is undisturbed, and then the fluorescence lifetime is τ_0. Thus, for static reaction $\tau_0/\tau=1$. In contrast, for dynamic reaction $F_0/F=\tau_0/\tau$. Meantime, the determination of time-resolved fluorescence lifetime can effectively avert the inner filter effect, because the lifetime measurements are comparatively independent of total fluorescence intensity.[18,19] In the relevant inquiries of fluorescence reaction, time-resolved fluorescence detections could thereby expose more concrete kinetic information regarding excited-state processes as compared with steady-state fluorescence, so that explaining exactly the bioreaction mechanism of fluorescence system. In the present experiments, the representative fluorescence decay patterns of protein at various molar ratios of (*R*)-/(*S*)-diclofop in Tris-HCl buffer, pH＝7.4, are exhibited in Fig. S2, and the fluorescence lifetime and their amplitudes are also collected in Table S2.

As we have seen, fluorescence lifetime of the chromophore is very sensitive about its circumjacent microenvironmental changes, and as a result, the determination of fluorescence lifetime alterations of the chromophore may aid in the examination of many phenomena during the biorecognition, for example, charge transfer, dipolar relaxation, molecular rotation, and quenching of the fluorophores. Obviously, the fluorescence decay curves fitted well to a biexponential function, and this event imply the presence of rotational isomers which might be connected with the lone electronic transition of fluorophore in equilibrium in the compact structure of protein.[20] It can be seen from Table S2 that the relative fluorescence lifetimes of protein are $\tau_1=3.42$ ns and $\tau_2=7.17$ ns ($\chi^2=1.04$), respectively, while in the maximum concentration of (*R*)-/(*S*)-diclofop, the relative fluorescence lifetimes of protein are $\tau_1=2.98/2.89$ ns and

τ_2＝6.78/6.55 ns (χ^2＝1.01/1.09), respectively. Undoubtedly, the biexponential decay of Trp residue originates from the dual emission from the ^1L_a and ^1L_b excited-states, and the existence of different rotamers, about the C^{α}-C^{β} or the C^{β}-C^{γ} bond of Trp residue was advocated by Szabo and Rayner[21] to supply the foundation for interpreting the biexponential decay. Detailedly, a fluorophore in a homogeneous environment is expected to reveal monoexponential fluorescence decay, whereas for the zwitterion of Trp residue, it is often found that a fluorophore has a biexponential decay pattern, and the molecular explanation could include either ground-state heterogeneity or excited-state reactions. More significantly, there is a single type of fluorophore in the current protein, ground-state heterogeneity may be elicited by the presence of multiple conformational states of the protein, which evokes the fluorophore to undergo a dissimilar environment and have a disparate decay time in each conformation.[22,23] In reality, because of steric effects between the side chain of the Trp residue and the backbone of the polypeptide chain, all rotamers are not utterly uniform. Upon the formation of the protein-diclofop enantiomers complexes, the quenching group nearest to the indole part is the small amino group, so such conformer has the largest population and the fluorescence lifetime is 7.17 ns. On the contrary, if the amino and carbonyl groups approach the indole ring, this rotamer might own the short fluorescence lifetime of 3.42 ns. And the discussion of conformers in protein is confined to the liquid solution, and the existence of diverse Trp residue rotamers has rigorously been confirmed via other experimental techniques such as nuclear magnetic resonance.[24] For this reason, the present task is not going to attempt to designate the respective component of fluorescence lifetime of the Trp-214 residue, instead the mean fluorescence lifetime has been utilized to qualitatively analyze the stereoselective biointeraction mechanism between the biomolecule and diclofop enantiomers.

It is evident to us that the average fluorescence lifetime of protein is 6.12 ns, which agree extremely with the former data reported by Abou-Zied and Al-Shihi[10] in a more recent contribution. At different concentrations of (*R*)-/(*S*)-diclofop, the average fluorescence lifetimes of protein change from 6.12 ns to 6.06/6.04 ns, $\tau_0/\tau \approx 1$, explicating plainly that the decrease of the Trp residue fluorescence intensity is principally controlled by static mechanism. Simultaneously, one can appreciably perceive that the average fluorescence lifetime express a shallow undulation, yet the amplitude is still in the tolerable range. Probably this phenomenon stem from the charge transfer from the indole ring in the Trp-214 residue to the adjacent substituent, which cause the slight enhancement on enantioselective bioreaction strength of the protein-chiral ligand and then lead to the marginally decline in the mean fluorescence lifetime. It is revelatory of a tiny contribution of dynamic behavior as only those

chiral ligands that experience dynamic reaction have been sole contribution in the shrink of the fluorescence lifetime. For that reason the time-resolved fluorescence energy transfer efficiency (E) computed from fluorescence lifetimes measurements exclusively symbolizes the energy transfer during the procedure of dynamic manner and is reaped according to the equation: $E=1-\tau/\tau_0$, where τ and τ_0 are the fluorescence lifetime of Trp residue in the presence and absence of (*R*)-/(*S*)-diclofop, respectively. The sizes of E calculated from time-resolved fluorescence data are detected to be 0.98%/1.31%, respectively, in the protein-diclofop enantiomers adducts at a molar ratio of protein to (*R*)-/(*S*)-diclofop of 1∶4. Apparently, the two data are very minute, hence we could fully think that the event of energy transfer is betided in the processes of chiral biorecognition, but the transfer efficiency is awfully low, almost negligible. These argumentations based on the data of time-resolved fluorescence accord wonderfully with the previous research findings of steady-state fluorescence, that is, stereoselective bioreaction of diclofop enantiomers with biopolymer is processed through static reaction in nature, or the formation of the noncovalent complexes between the protein and chiral ligand, and the binding domain of chiral diclofop is located in the vicinity of the Trp-214 residue (subdomain IIA), thereby arousing some changes in the spatial conformation of protein.

We really should point out that even the conformational transition of the functional protein may be triggered by diclofop enantiomers, however, multiexponential fluorescence decay behavior might be attributed to the different conformations of protein rather than an allotment to diverse Trp residues in a protein of one conformation at neutral pH.[25,26] In the meantime, the impacts of (*R*)-/(*S*)-diclofop on the fluorescence lifetime of the protein chromophore have distinct differences, manifesting the molecular recognition of the biomolecule-chiral compound possess pretty enantioselectivity, and such stereochemical property has disparate influence on the chiral biointeraction features such as bioreaction strength, conformational alteration and thermodynamic function. These experimental results narrated above are consistent with the careful interpretation based upon circular dichroism and molecular modeling, and a parallel story has been depicted very recently by Abou-Zied[27] for the explanation of the bioreaction between hydroxypyridines, hydroxyquinolines and hydroxyphenyl benzazoles and albumin by exploiting steady-state and time-resolved fluorescence and UV/vis absorption spectroscopy.

Strength and Stoichiometry of Enantioselective Bioreaction. As set forth, biological activities of chiral substance shall be achieved through the severely chiral matching and molecular recognition with biomacromolecule, that is to say, via interacting with the receptor, which has specific physical form, chiral chemical can

exert physiological actions in the human body. In general, the optical isomers of chiral agent bind to biological macromolecule, and form the diastereoisomeric bioconjugates with different characteristics and appear the disparities in biorecognition strength, and then bring on the stereoselective characters of chiral chemical in the body and finally produce the enantiomeric discrepancies in pharmacological/toxicological properties. We could therefore appreciate that the understanding of bioreaction intensity of chiral recognition is vitally important to scrutinize the enantioselective biointeraction variations of chiral compound with biomacromolecule.

Steady-state and time-resolved fluorescence data implied patently that the biorecognition strength between protein and diclofop enantiomers has considerable difference. To definitely clarify such stereochemical phenomenon, equation (7) was used to handle the steady-state fluorescence intensity of protein in the presence of different concentration of (*R*)-/(*S*)-diclofop by a plot of the $\log(F_0-F)/F$ *against* log[*Diclofop Enantiomers*], and the bioreaction strength and stoichiometry of the stereoselective biointeractions at different temperatures is displayed in Table S3. Visibly, the biorecognition intensity *K* is shortened with the rising temperature, which stated clearly that the noncovalent bioconjugates are shaped between protein and chiral diclofop through weak interactions, and the complexes will partly be decomposed when the temperature elevated, so that engendering the abasement of *K* value. In the light of the viewpoint of Dufour and Dangles,[28] together with the recently related inquisitions with respect to the molecular recognition of the protein-ligand, e.g. chalcone derivative, emodin, gold/silver alloy nanoparticles, L-3,4-dihydroxyphenylalanine, lomefloxacin, metal-quinolone, neutral red, piperamides, retinol and retinoic acid,[13,29-36] one may notice smoothly that the bioreaction strength of the enantioselective biorecognition of diclofop enantiomers with protein falls within the ambit of moderate association, because other forceful protein-ligand recognition normally has the biointeraction intension ranging from $10^6\sim10^8$ M^{-1}. Further, Table S3 also displays that the stoichiometry of the chiral bioreaction of the protein-(*R*)-/(*S*)-diclofop is $n\approx1$, directing the presence of only one kind of binding site in protein molecule for chiral chemical. According to the results of X-ray diffraction crystallography,[37] and combined with the nomenclature of Sudlow et al.,[38,39] we found that the globular protein used in the present endeavor has chiefly two ligand binding domain, subdomains IIA and IIIA, and the fluorescent Trp residue lie at the position 214 along the amino acid sequence of the polypeptide chain, which should be geared to subdomain IIA. As might lucidly be known from the foregoing experimental results of steady-state and time-resolved fluorescence, chiral diclofop can give rise to the outstanding falloff of the fluorescence intensity of the aromatic

residue, hinting that diclofop enantiomers are located at the proximity of the Trp-214 residue, namely subdomain IIA. Significantly, although (*R*)-/(*S*)-diclofop situate within the same binding region on protein, the biorecognition intensity of (*S*)-diclofop with protein is nearly 1.7 times larger than (*R*)-diclofop, which link inseparably with the chiral stamp of bioactive diclofop. Or rather, owing to the intrinsic chiral earmark of biomolecules, the dissimilar enantioselectivity could surely be represented macroscopically when they recognize the optical isomers of chiral agent, in order to effectuate the sternly chiral matching. Incontestably, such phenomena further testify the analytical outcomes of both steady-state and time-resolved fluorescence, viz. stereoselectivity make paramount contribution to the enantioselective biointeraction processes between biomacromolecule and chiral compound.

Physiologically, after the racemic substances such as drugs and pesticides enter the human body, several crucial biochemical and physiological processes, e.g. absorption, bioavailability, distribution, excretion, metabolism, transformation and transportation need to be interfered with the key biopolymers; thus these life activity bioprocesses are tightly associated with the stereoselective biorecognitions (particularly bioreaction strength) between endogenous biomolecules and chiral agents to a large extent.[40-42] For instance, because of the impact of enantioselectivity, one enantiomer may reversibly be bound highly to plasma proteins or egested/metabolized rapidly upon the racemic drugs absorbed by the body, and possibly it is hard to pass blood-brain barrier and arrive at the site of action on the central nervous system, or interact with other biosystems so as to produce adverse effects. However, the plasma protein-enantiomer adducts with high affinity might maintain stable plasma drug concentration by the controlled release of drug enantiomer for a long time, and ultimately affect the total pharmacokinetic properties of the racemic drugs, e.g. clearance and volume of distribution. It follows that the stereoselectivity behave in the wholly biological processes of chiral compounds in the organism, and the subtle distinctions of chiral biointeraction, for example, the discrepancies of the maximum bioreaction capacity and affinity between biomolecule and ligand enantiomers, can likely create the notable differences in pharmacological/toxicological effects of ligand enantiomers for the human body. This requires that we ought to sufficiently consider biochirality and stereochemistry when elaborate chiral chemicals, so that appraising accurately the biological activities and physiological actions of chiral substances in the asymmetric environment of the body.

Biointeraction Cavity of Isomeric Diclofop. Under the fluorescence essay data of biomacromolecule, one could savvy intelligibly that the biorecognition area of chiral diclofop is located at the subdomain IIA on protein. To validate such conclusion, the following will utilize denaturation of protein, hydrophobic fluorescent

molecule displacement and site-specific competitive experiments to exactly expound the binding patch of (*R*)-/(*S*)-diclofop on the typical protein. First of all, the assays of protein denaturation were employed to illustrate the concrete binding area of chiral ligand on biopolymer. Routinely, there are several approaches to unfold a protein according to the damage of the noncovalent bonds, i.e. hydrogen bonds, hydrophobic effects, π-π stacking and van der Waals forces that keeps the protein folded, and the most frequently used method is chaotropic agents such as guanidine hydrochloride (GuHCl) and urea, except for heating, strong acids, strong bases and ultraviolet radiation. In the present experiment, the denaturant, GuHCl, has been exploited to process the chemical denaturation examination for model protein.

As Ahmad et al.[43] have stated, GuHCl induced albumin unfolding to take place in multiple steps, at 1.4 M GuHCl, only domain III is completely unfolded, the presence of a molten globule-like intermediate state of domain III is around 1.8 M GuHCl concentration and at 3.2 M GuHCl, domain I is departed from the domain II, domain I is fully unfolded while domain II is partly. This unfolding action has been affirmed by Galantini et al.,[44] who explored a small-angle X-ray scattering and light scattering techniques to illuminate the unfolding cartoon of fatted and defatted albumin. Under the circumstances, samples of different GuHCl were prepared by blending varied molar ratios of GuHCl stock solution and Tris-HCl buffer of pH＝7.4. The final solution mixture was incubated with various GuHCl concentrations for 12 h at room temperature before fluorescence emission determinations. Relative to the hydrophobic environment, the quantum yield of the aromatic residues reduces leading to low fluorescence intensity in a hydrophilic environment (exposed to solvent). Particularly, there is forceful Stokes shift for Trp residue in albumin relies on the solvent, suggesting that the maximum fluorescence emission wavelength of Trp residue will diverge counting on the residue microenvironment (data not shown). The relationship equation (7) was used to treat the steady-state fluorescence effects of protein Trp residue by chiral diclofop in the existence of different concentrations of GuHCl (0, 1.4, 1.8, and 3.2 M), and the bioreaction intensities (298 K) were observed to be 1.403/2.371, 1.291/2.015, 1.025/1.669, and 0.06917/0.05296$\times10^4$ M^{-1} for the protein-(*R*)-/(*S*)-diclofop, respectively. Evidently, chiral biointeraction strengths have varying degrees of reduction in the presence of GuHCl, which enunciated that the three-dimensional conformation of protein consisted of the hover of polypeptide chain own the spatial order, and all functional binding domains are correlative dependence. It is worthwhile to note that the bioreactivity extent between globular protein and chiral diclofop is the lowest, alluding that the partial unfolding of domain II has the biggest influence on such enantioselective biorecognition, namely domain II hold high affinity for (*R*)-/(*S*)-diclofop.

Ideally, hydrophobic 8-anilino-1-naphthalenesulfonic acid (ANS) is one of the most frequently used fluorescent chemicals for the examination of nonpolar sites in proteins, and in 1966 ANS fluorescence was efficaciously employed to characterize five hydrophobic domains on bovine serum albumin.[45] At present, ANS is extensively utilized as a reporter of nonpolar surface pockets of proteins or as a back titration fluorescence indicator for lipid ligand displacement from lipid transporter proteins or, in general, analysis of protein structural features.[46-48] To firmly reconnoiter the bioreaction region of chiral diclofop on protein, the tests of stereoselective biointeractions were conducted in the presence of ANS under the identical conditions, and the relative fluorescence intensity (F/F_0) *versus* ligand concentration ([Ligand]) plots is displayed in Fig. S3.

It is quite conspicuous that both (*R*)-/(*S*)-diclofop and ANS drop clearly the steady-state fluorescence intensity of the chromophore in protein at the chiral ligand concentration of 18 μM, but the extent of fluorescence slump has relatively large disparity. Specifically, ANS might quench 77.59%, while (*R*)-/(*S*)-diclofop can just lower 24.37%/28.58% of Trp residue fluorescence emission intensity. In a very early study, Stryer[49,50] first discovered that the quantum yield of free ANS in water is about 0.004 and becomes as high as 0.98 when the dye molecules are bound to apomyoglobin. And he has also set up that the fluorescence of ANS bound to the nonpolar sites of apomyoglobin and apohemoglobin was equal to the fluorescence of an equivalent mass of ANS in a number of hydrophobic organic solvents. Hence, when chiral diclofop is joined in the ANS-protein complex, it could rival ANS for the hydrophobic domain on protein molecule, bringing on the shrinkage of the fluorescence intensity in the ANS-protein. It is apparent from Fig. S3 that the fluorescence intensity of the ANS-protein adducts shortened about 17.54%/18.03% in the maximal amounts (18 μM) of (*R*)-/(*S*)-diclofop, which evinces that diclofop enantiomers and hydrophobic ANS have somewhat weakly competitive binding reactions in functional protein. There have already many reports regarding the explorations of the definitive binding area of ANS probe on protein.[51-56] Although still partly controversial, consensus exists today that there are four hydrophobic binding sites for ANS associated with albumin, but preferentially at a site in subdomain IIIA. In the current experimental conditions, approximately 17.54%/18.03% displacement of ANS molecule may be sighted from the corresponding binding patch by (*R*)-/(*S*)-diclofop, respectively, which testifies that the dominant biorecognition pockets of chiral diclofop and fluorescent ligand ANS in protein are not overlapped. In other words, the binding domain of (*R*)-/(*S*)-diclofop on globular protein is located at subdomain IIA (Sudlow's site I), whereas the complexed ANS is chiefly situated within subdomain IIIA, and no intensely competitive binding relations might be seen

between the two ligands, so the steady-state fluorescence intensity of the ANS-protein bioconjugates was noticeably unaffected. Undeniably, such verdict accords with the former findings based on the protein denaturation induced by denaturant GuHCl, and also match the site-specific competitive experiments by utilizing the classical site labeling ligand as the protein marker in the next section.

This part of the tale shall thoroughly verify the bioreaction zone of (*R*)-/(*S*)-diclofop on the typical protein via the application of the specific ligand competitive assays. The pioneering effort of Sudlow et al.[38,39,52] of competitive binding studies established site I and site II as a discrete locus for certain drugs, with 5-dimethylaminonaphthalene-1-sulfonamide and dansylsarcosine as two markers, but did not assign they to the region of the protein molecule. Fortunately, the X-ray diffraction crystallographic findings of Carter's group showed the binding cavity corresponding to site I and site II to lie in subdomains IIA and IIIA,[37,57] respectively. Structurally, site I is known as the warfarin-azapropazone site, and shaped as a pocket in subdomain IIA, the lone Trp-214 residue of protein in this region. The inside wall of the domain is formed by hydrophobic side chains, while the entrance to the orifice is surrounded by positively charged residues. And similarly, site II corresponds to the cavity of subdomain IIIA, and is also known as the indole-benzodiazepine site, which is almost the same size as site I, the interior of the hole is constituted by hydrophobic residues and the exterior patch presented two significant residues, i.e. Arg-410 and Tyr-411. As a role, site I ligands are bulky heterocyclic anions with the charge situated in a fairly central position in the molecule. This differentiates them from the ligands typical of site II, located in domain IIIA, which are generally aromatic and can be neutral; a charge, if present, is anionic and located more peripherally on the molecule.[58] Now so many different compounds are believed to bind in the region termed site I and site II by Sudlow et al. that they would be considered here together despite their great diversity. Many of them are therapeutic drugs, for example, azapropazone, indomethacin, phenylbutazone and warfarin are among the site I drugs,[59-61] whereas site II drugs includes clofibrate, diazepam, flufenamic acid and naproxen.[62] Later, supporting biochemical evidences of Kragh-Hansen, Brodersen's and Tillement's groups found that digitoxin is distinct from both of the two Sudlow's sites, and perch on what was nominated as site III.[63-65] Therefore the competitors used in this essay included warfarin, a classical marker for site I, diazepam for site II, digitoxin for site III and hemin for domain I.

According to the protocol, we measured the enantioselective biointeractions between the protein and chiral diclofop in the presence of different competitive agents, and the linear equation (7) was applied to deal with fluorescence experiment data, and the chiral biorecognition strengths of the protein-(*R*)-/(*S*)-diclofop were determined to

be 1.403/2.371, 0.2918/0.3144, 1.335/2.173, 1.289/2.287, and 1.252/2.205×10^4 M^{-1} for blank, warfarin, diazepam, digitoxin, and hemin, respectively. Clearly, the stereoselective bioreaction of the protein-chiral diclofop was most inhibited by warfarin, thereby sparking off the biomacromolecule-chiral compound possess the smallest biointeraction intensity. This signifies immovably that both (*R*)-/(*S*)-diclofop and warfarin might competitive bind to the same biorecognition region on protein, i.e. they have the uniform ligand binding location, subdomain IIA (Sudlow's site I).

Conformational Transition of Biomolecule. Fluorescence experiments disclosed that the enantioselective bioreaction of chiral diclofop by protein could lead to the descent of the emission intensity of the chromophore, insinuating that some changes occurred in the spatial conformation of protein, as a conformational alteration of a biomolecule induced by ligand biorecognition may frequently cause a variation of the fluorescence intensity.[15] Simultaneously, research outcomes of biointeraction domain stated certainly that both (*R*)-diclofop and (*S*)-diclofop are situated at subdomain IIA on protein, Sudlow's site I, and this is another convincingly proof to the conformational changes. Ordinarily, conformational alterations in the present globular protein are evident with many site I ligands. This phenomenon was taken to mean that the "configurational adaptability" involves more than the immediate vicinity of a ligand and might affect the compactness or decompaction of structure of the whole protein molecule.[66]

To quantitative weigh the structural changes of protein during the stereoselective biorecognition of the biopolymer-chiral agent, the far-UV CD spectra (Fig. S4) of protein with different concentrations of (*R*)-/(*S*)-diclofop were scanned and secondary structure contents received on the basis of raw CD data listed in Table S4. It is palpably that the CD curve of the pure protein expressed two negative peaks in the far-UV region at 208 nm and 222 nm (negative Cotton effect), which are the typical characteristic of the α-helical structure of globular protein.[67,68] A rational explanation for this phenomenon is that the negative peaks between 208 nm and 209 nm and 222 nm and 223 nm are dominated through both $n\rightarrow\pi^*$ and $\pi\rightarrow\pi^*$ transitions of amide groups and are also affected by the geometries of the polypeptide backbones.[69,70] Table S4 communicates free protein embraces 56.9% α-helix, 8.5% β-sheet, 10.8% turn and 23.8% random coil; upon binding with diclofop enantiomers, a reduction of α-helix was noted from 56.9% (free protein) to 51.1%/48.3% (protein-(*R*)-/(*S*)-diclofop), and furthermore, there was an ascension in β-sheet, turn and random coil from 8.5%, 10.8% and 23.8% (free protein) to 9.4%/9.5%, 12.4%/12.9% and 27.1%/29.3% (protein-(*R*)-/(*S*)-diclofop) at a molar ratio of protein to diclofop stereoisomers of 1∶4. It was without a shadow of a doubt the contraction of α-helical fraction with an increment in the β-sheet, turn and random coil segment declared

crisply chiral diclofop yields noncovalent bonds with amino acid residues of the polypeptide chain and resulting in the destabilization of the orderly spatial conformation in protein molecule, e.g. some extent of structural extension of the protein occurred upon bioreaction with diclofop enantiomers. Moreover, we can also awake from Table S4 that the impact of (*S*)-diclofop on secondary structures of protein is higher than (*R*)-diclofop, and presumably, it could be because the biorecognition strength of (*R*)-diclofop with protein is lower than (*S*)-diclofop, that is, strongly noncovalent bonds are formed between (*S*)-diclofop and the important residues, and thus such issue has somewhat great influence on the regularly spatial conformation of protein. This event further authenticate the biointeraction happened in the human body is designed to possess the enantioselectivity when endogenous biomacromolecule face chiral chemical, and then the (*R*)-/(*S*)-enantiomers may generate different effects on the structure of biological macromolecule; yet the structure of biomolecule is related intimately to its biological function, and thereby these optical isomers might finally be exhibited various biological activities in living organisms.

Thermodynamic Functions of Chiral Biorecognition. Biologically, the amino acid sequence of protein is dictated by covalent bonds, but the higher levels of structure – secondary, tertiary, and quaternary are formed and stabilized by weak, noncovalent interactions. Electrostatic interactions, hydrogen bonds, hydrophobic effects and van der Waals forces are all noncovalent in nature, yet they are extremely important influences on protein conformation.[71] The aforementioned analytical results of fluorescence and CD spectra announced memorably that chiral compound may evoke the significant alterations in the orderly spatial conformation of biomolecule, viz. chiral bioreaction of the protein-diclofop enantiomers perturbed the noncovalent bonds which maintain the three-dimensional conformation of protein. The stabilization free energies afforded by each of these biointeractions might be highly dependent on the local microenvironment within the protein, but certain generalizations can still be made. According to the classical van't Hoff relationship, we will pry into the thermodynamic functions of the biopolymer-ligand enantiomers during the chiral biorecognition, in order to seek the pivotal noncovalent bonds in the enantioselective bioreaction of the biomolecule-chiral substance, and further clarify the thermodynamic influences and disparities of stereoselectivity on the biointeractions of the chiral biosystems. Physicochemically, thermodynamic functions could offer insight into the energetics of biomacromolecule-ligand bioreactions that is not readily attainable by other means. The utility of thermodynamic analysis has traditionally been considered more the domain of chemistry than biology. However, the modern biorecognition of an interface in the case of biopolymer-ligand

biointeractions, particularly when the biological macromolecule is a protein or a target receptor, has kindled an integration with pragmatic benefit to basic understanding and to enantiomeric biorecognition efforts. Usually, the energetics of bioreactions in solution is expressed in terms of three functions: $\Delta G°$, the Gibbs free energy; $\Delta H°$, the enthalpy; and $\Delta S°$, the entropy. As set forth, there are four types of noncovalent bonds existing in ligand binding functional biomolecules, that is electrostatic interaction, hydrogen bond, hydrophobic effect and van der Waals force. The sign and magnitude of thermodynamic functions for protein biorecognitions may interpret the acting forces donated to protein stability. Suppose the enthalpy $\Delta H°$ does not change conspicuously over the temperature scope examined, then the three thermodynamic functions are allied by equations (9) and (10):[72,73]

$$\ln K = \frac{-\Delta H^{\circ}}{RT} + \frac{\Delta S^{\circ}}{R} \tag{9}$$

$$\Delta G^{\circ} = \Delta H^{\circ} - T\Delta S^{\circ} \tag{10}$$

In these expressions K is the bioreaction strength for a given event of biomolecular recognition under a specified set of experimental conditions, R is the gas constant, T is the absolute temperature, and the superscript "°" displays the data of the property of a molar concentration of unity. A linear plot Fig. S5 of ln$K$ *against* 1/T creates $\Delta H°$ and $\Delta S°$, and the outcomes fitted from Fig. S5 were also pooled in Table S3. It was obvious that enantioselective biorecognition of the protein-chiral molecule is spontaneous in the forward direction and energy is released due to the Gibbs free energy $\Delta G° < 0$. In a relatively early review, Ross and Subramanian[74,75] have epitomized the sign and magnitude of the thermodynamic functions related to various individual types of bioreaction that might occur in biomacromolecule biointeraction processes, as recounted below. From the point of view of solvent structure (usually water solution), a positive $\Delta S°$ value is frequently taken as a typical proof for hydrophobic effect, and the negative $\Delta H°$ value observed might not be mostly ascribed to electrostatic interaction, as electrostatic interaction $\Delta H°$ is very small, almost zero. A negative $\Delta H°$ value is often detected whenever there are hydrogen bonds in the biomolecular recognition. And it is something inappropriate to account for the thermodynamic functions of a protein-ligand bioreaction system in the light of a single intermolecular force model. With regard to the current chiral recognition biosystems, it can straightforwardly be known from Table S3 that the enthalpy changes ($\Delta H°$) and the entropy changes ($\Delta S°$) of the stereoselective biorecognitions are less than zero, i.e. the $\Delta H° = -49.29/-49.11$ kJ mol^{-1} and $\Delta S° = -85.72/-80.55$ J mol^{-1} K^{-1} for the protein-(*R*)-isomer and the protein-(*S*)-isomer, respectively, which elucidates definitely that both hydrogen bonds and van der Waals force play a

leading role in the chiral biointeraction of the biopolymer-diclofop stereoisomers. At the same time, it is worth noting that the two chiral biosystems, namely the biomacromolecule-(*R*)-enantiomer and the biomolecule-(*S*)-enantiomer have certain differences in thermodynamic functions, and these chiral biorecognition discrepancies in thermodynamics are correspondent highly with the comparable research findings of molecular modeling (free energy decomposition). Or rather, such disparity derives distinctly from the enantioselectivity of the stereoselective bioreaction processes between the biological macromolecule which retain the unique three-dimensional spatial conformation and chiral chemical.

Overall Energy Analysis. The Lennard-Jones potential is an effectively mathematical model that can be employed to scratch the energy of crucial biointeraction of the biomacromolecule-chiral compound during the dynamic stereoselective recognition, and the Coulomb potential is an applicable pair potential that narrates the interaction between two point charges, this parameter could often be used to unravel the electrostatic interaction in chiral bioreaction.[76,77] Both the Lennard-Jones potential and the Coulomb potential of the protein-diclofop enantiomers are collected in Table S5, it is perceptibly to us that the capital energy contributions of the chiral systems stems from Coulomb term, and the data of Coulomb energy are found to be -17.91 kJ mol^{-1} and -22.46 kJ mol^{-1} for the protein-(*R*)-diclofop and protein-(*S*)-diclofop bioconjugates, respectively; while the energy contributions of Lennard-Jones term are somewhat weak, which certifies outstandingly that electrostatic interaction energy play a major role in total energy. Furthermore, contrasted the Coulomb energy in Table S5 with the electrostatic energy in Table 1, one may easy discern that the computed outcomes have a preferable consistency. Besides, the total energies of the biomolecule-(*R*)-/(*S*)-diclofop systems are calculated based upon the Lennard-Jones potential and the Coulomb potential, and the available values are respectively -23.55 kJ mol^{-1} and -28.16 kJ mol^{-1}, which dovetails excellently with the experimental findings in aqueous solution. Doubtlessly, these biological issues testify that the energy discussions are logically reasonable in the current research.

Table S1. Stern-Volmer and bimolecular quenching parameters for the stereoselective biorecognition of diclofop enantiomers with protein

Biosystems	T (K)	K_{SV} ($\times 10^4$ M^{-1})	k_q ($\times 10^{12}$ M^{-1} s^{-1})	R^a
Protein＋(*R*)-diclofop	298	1.656	2.706	0.9994
	302	1.609	2.629	0.9998
	306	1.523	2.489	0.9996
	310	1.412	2.307	0.9996
Protein＋(*S*)-diclofop	298	2.116	3.458	0.9994
	302	1.909	3.119	0.9996
	306	1.768	2.889	0.9995
	310	1.677	2.740	0.9984

[a] R is the correlation coefficient.

Table S2. Time-resolved fluorescence lifetime of protein (10 μM) as a function of concentrations of diclofop isomers

Samples	τ_1 (ns)	τ_2 (ns)	A_1	A_2	τ (ns)	χ^2
Free protein	3.42	7.17	0.28	0.72	6.12	1.04
Protein＋(*R*)-diclofop (1∶1)	3.23	7.05	0.26	0.74	6.06	0.99
Protein＋(*R*)-diclofop (1∶2)	3.11	6.94	0.24	0.76	6.02	1.08
Protein＋(*R*)-diclofop (1∶4)	2.98	6.78	0.19	0.81	6.06	1.01
Protein＋(*S*)-diclofop (1∶1)	3.11	6.95	0.24	0.76	6.03	0.98
Protein＋(*S*)-diclofop (1∶2)	3.04	6.76	0.19	0.81	6.05	1.05
Protein＋(*S*)-diclofop (1∶4)	2.89	6.55	0.14	0.86	6.04	1.09

Table S3. Enantioselective biointeraction parameters and thermodynamic functions for the protein-diclofop stereoisomers biosystems at different temperatures

Biosystems	T (K)	K ($\times 10^4$ M^{-1})	n	R^a	$\Delta H°$ (kJ mol^{-1})	$\Delta G°$ (kJ mol^{-1})	$\Delta S°$ (J mol^{-1} K^{-1})
Protein＋	298	1.403	0.98	0.9989	－49.29	－23.66	－85.72
(*R*)-diclofop	302	1.138	0.98	0.9991		－23.45	
	306	0.9419	0.97	0.9991		－23.28	
	310	0.6339	0.95	0.9997		－22.56	
Protein＋	298	2.371	1.01	0.9989	－49.11	－24.96	－80.55
(*S*)-diclofop	302	2.075	1.01	0.9991		－24.96	
	306	1.570	1.00	0.9986		－24.58	
	310	1.107	0.98	0.9995		－24.00	

[a] R is the correlation coefficient.

Table S4. Secondary structure components of protein (10 μM) stereoselective bioreaction with diclofop enantiomers at pH＝7.4 assessed by Jasco Spectra Manager II Software

Samples	Secondary structure constituents (%)			
	α-Helix	β-Sheet	Turn	Random
Free protein	56.9	8.5	10.8	23.8
Protein＋(*R*)-diclofop (1：2)	54.2	8.9	11.7	25.2
Protein＋(*R*)-diclofop (1：4)	51.1	9.4	12.4	27.1
Protein＋(*S*)-diclofop (1：2)	52.4	9.1	11.8	26.7
Protein＋(*S*)-diclofop (1：4)	48.3	9.5	12.9	29.3

Table S5

Interaction energies (kJ mol^{-1}) of the protein-diclofop enantiomers bioconjugates

Chiral biosystems	Lennard-Jones energy	Coulomb energy	Total energy
Protein-(*R*)-diclofop	−5.64	−17.91	−23.55
Protein-(*S*)-diclofop	−5.70	−22.46	−28.16

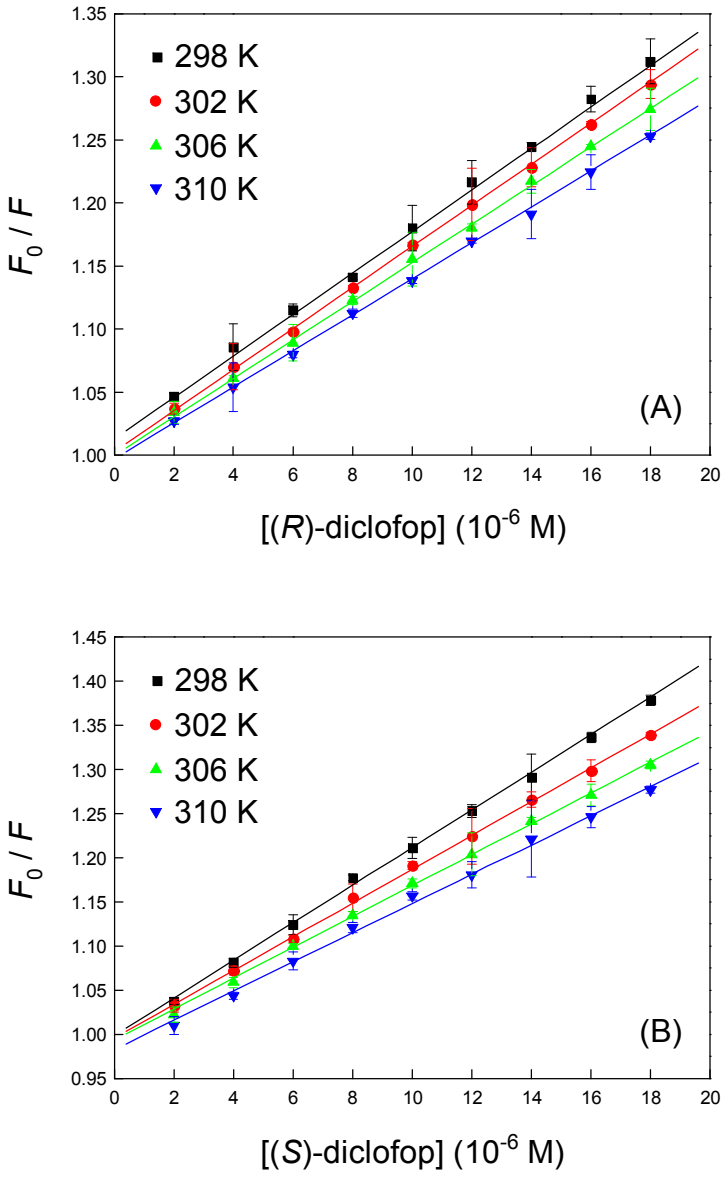

Fig. S1. Stern-Volmer plot narrating fluorescence bioreaction of protein (1.0 μM) at pH＝7.4 in the presence of different concentrations of (*R*)-diclofop (panel (A)) and (*S*)-diclofop (panel (B)), respectively. Fluorescence emission intensity was gathered at λ_{ex}＝295 nm, and the λ_{em} maximum occurred at 333 nm. All data were corrected for diclofop enantiomers fluorescence, and each point was the mean of three separate determinations±S.D. ranging 0.63%－4.33%.

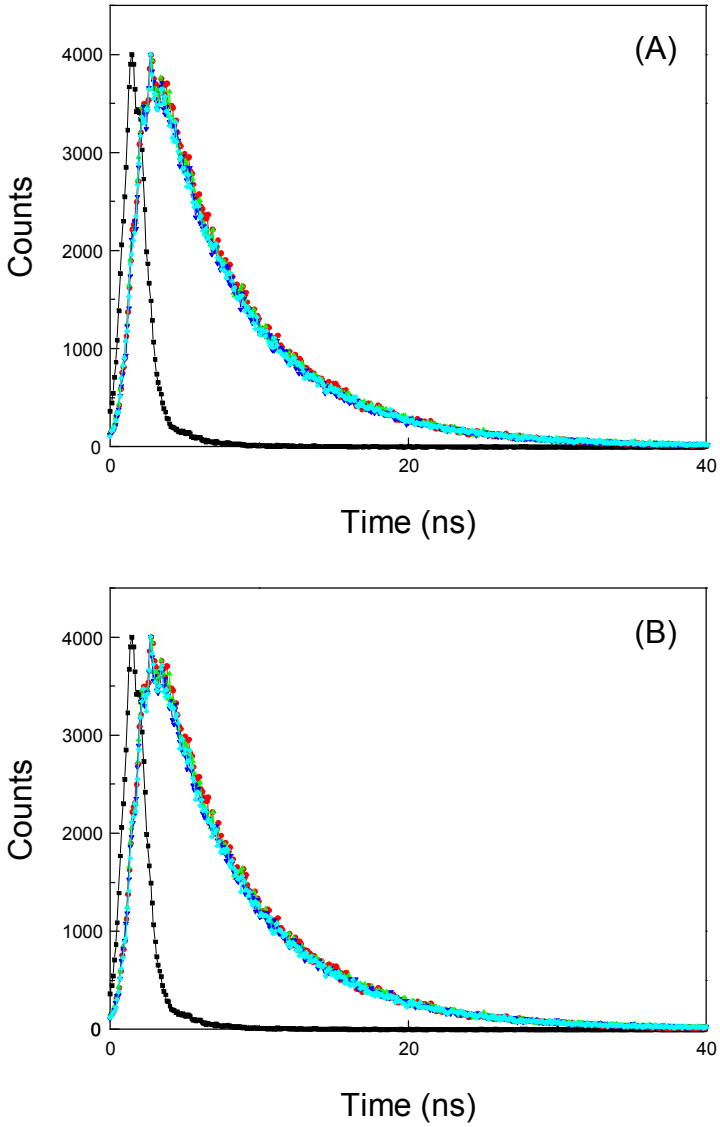

Fig. S2. Time-resolved fluorescence decays of protein in Tris-HCl buffer (pH＝7.4) as a function of the amounts of (*R*)-diclofop (panel (A)) and (*S*)-diclofop (panel (B)), respectively. *c*(protein)＝10 μM, *c*(diclofop isomers)＝0 (red), 10 (green), 20 (blue) and 40 (cyan) μM. The sharp pattern on the left (black) is the lamp profile.

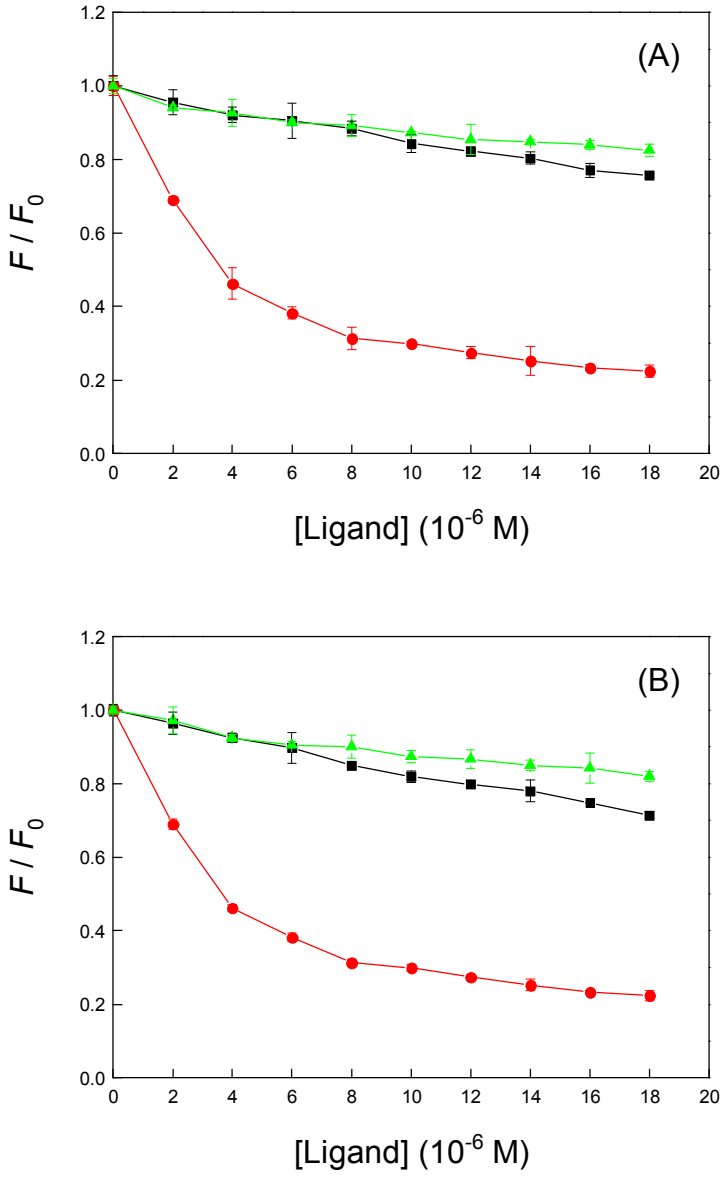

Fig. S3. Fluorescence decrease effects of proteins and ANS-protein bioconjugates at pH＝7.4 and *T*＝298 K; panel (A): protein-(*R*)-diclofop; and panel (B): protein-(*S*)-diclofop. The decline extent of diclofop stereoisomers (■) and ANS (●) induced drop of Trp residue fluorescence and fall of ANS-protein adduct fluorescence by diclofop enantiomers (▲). Each data was the average of three independent experiments±S.D. ranging 0.14%－4.76%.

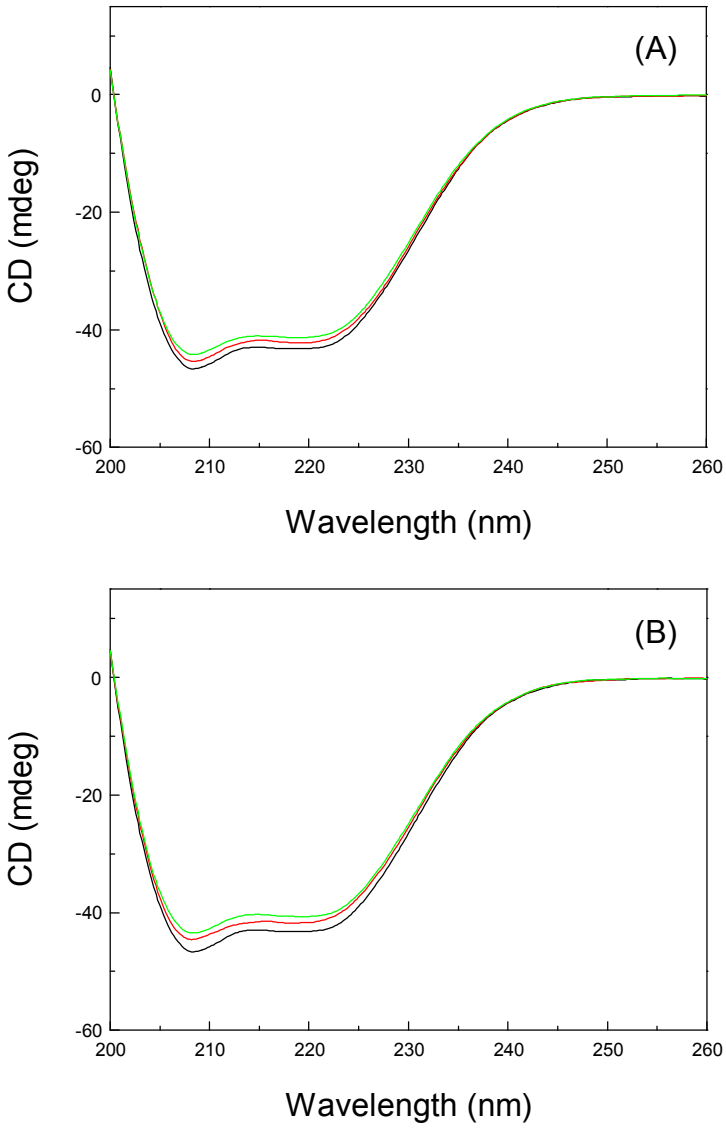

Fig. S4. Far-UV CD spectra of the protein-diclofop enantiomers complexes at pH＝7.4 and T＝298 K, 10 μM protein in the existence of 0 (black), 20 (red) and 40 (green) μM diclofop isomers; panel (A): (*R*)-diclofop; and panel (B): (*S*)-diclofop.

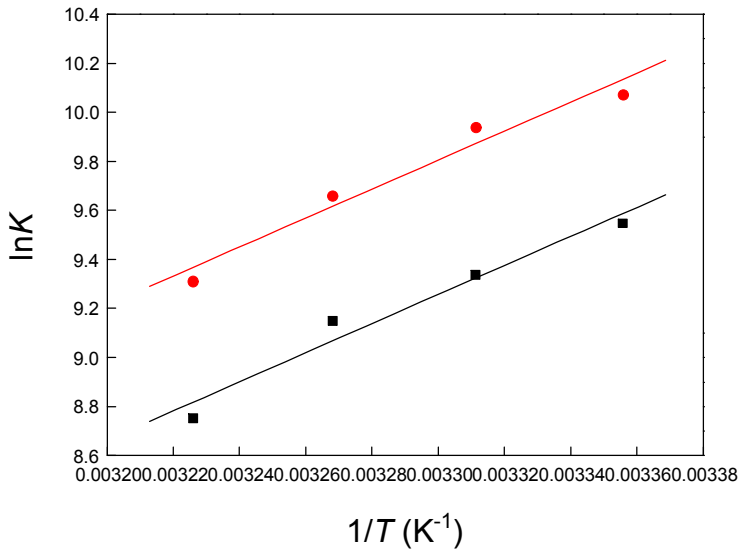

Fig. S5. van't Hoff plot for the enantioselective biorecognition of the protein-(*R*)-diclofop (black) and protein-(*S*)-diclofop (red) biosystems in Tris-HCl buffer, pH＝7.4.

Supplementary References:

1. O. H. Lowry, N. J. Rosebrough, A. L. Farr and R. J. Randall, *J. Biol. Chem.*, 1951, **193**, 265-275.
2. J. R. Lakowicz, in *Principles of Fluorescence Spectroscopy*, Springer Science+ Business Media, New York, NY, 3rd edn., 2006.
3. S. Sugio, A. Kashima, S. Mochizuki, M. Noda and K. Kobayashi, *Protein Eng.*, 1999, **12**, 439-446.
4. M. J. D. Powell, *Comput. J.*, 1964, **7**, 155-162.
5. S. J. Weiner, P. A. Kollman, D. A. Case, U. C. Singh, C. Ghio, G. Alagona, S. Profeta Jr. and P. Weiner, *J. Am. Chem. Soc.*, 1984, **106**, 765-784.
6. J. Gasteiger, *Nat. Chem.*, 2015, **7**, 619-620.
7. J. E. Kerrigan, in *In Silico Models for Drug Discovery*, ed. S. Kortagere, Springer Science+Business Media, New York, NY, 2013, vol. 993, pp 95-113.
8. J. Weiser, P. S. Shenkin and W. C. Still, *J. Comput. Chem.*, 1999, **20**, 217-230.
9. O. Stern and M. Volmer, *Phys. Z.*, 1919, **20**, 183-188.
10. O. K. Abou-Zied and O. I. K. Al-Shihi, *J. Am. Chem. Soc.*, 2008, **130**, 10793-10801.
11. S. K. Ahmadi, M. M. Moghadam, P. Mokaberi, M. R. Saberi and J. Chamani, *J. Biomol. Struct. Dyn.*, 2015, **33**, 1880-1898.
12. L. B. Devi, S. K. Das and A. B. Mandal, *J. Phys. Chem. C*, 2014, **118**, 29739-29749.
13. A. S. Sharma and M. Ilanchelian, *J. Phys. Chem. B*, 2015, **119**, 9461-9476.
14. M. P. Brown and C. Royer, *Curr. Opin. Biotechnol.*, 1997, **8**, 45-49.
15. R. Hovius, P. Vallotton, T. Wohland and H. Vogel, *Trends Pharmacol. Sci.*, 2000, **21**, 266-273.
16. K. K. Ding, H. X. Zhang, H. F. Wang, X. Lv, L. M. Pan, W. J. Zhang and S. L. Zhuang, *J. Hazard. Mater.*, 2015, **299**, 486-494.
17. S. L. Zhuang, H. F. Wang, K. K. Ding, J. Y. Wang, L. M. Pan, Y. L. Lu, Q. J. Liu and C. L. Zhang, *Chemosphere*, 2016, **144**, 1050-1059.
18. I. Hemmilá and V.-M. Mukkala, *Crit. Rev. Clin. Lab. Sci.*, 2001, **38**, 441-519.
19. J. A. Ross and D. M. Jameson, *Photochem. Photobiol. Sci.*, 2008, **7**, 1301-1312.
20. J. M. Beechem and L. Brand, *Annu. Rev. Biochem.*, 1985, **54**, 43-71.
21. A. G. Szabo and D. M. Rayner, *J. Am. Chem. Soc.*, 1980, **102**, 554-563.
22. M. R. Eftink, in *Methods of Biochemical Analysis, Volume 35: Protein Structure Determination*, ed. C. H. Suelter, John Wiley & Sons, Inc., Hoboken, NJ, 1991, pp 127-205.
23. M. R. Eftink, Y. W. Jia, D. Hu and C. A. Ghiron, *J. Phys. Chem.*, 1995, **99**, 5713-5723.
24. O. Julien, G. L. Wang, A. Jonckheer, Y. Engelborghs and B. D. Sykes, *Proteins: Struct., Funct., Bioinform.*, 2012, **80**, 239-245.
25. F. R. Beierlein, O. G. Othersen, H. Lanig, S. Schneider and T. Clark, *J. Am.*

Chem. Soc., 2006, **128**, 5142-5152.
26. O. J. Rolinski, K. Scobie and D. J. S. Birch, *Phys. Rev. E Stat. Nonlin. Biol. Soft Matter Phys.*, 2009, **79**, 050901.
27. O. K. Abou-Zied, *Curr. Pharm. Des.*, 2015, **21**, 1800-1816.
28. C. Dufour and O. Dangles, *Biochim. Biophys. Acta – Gen. Subj.*, 2005, **1721**, 164-173.
29. M. K. Prashanth, H. N. Deepakumari, M. S. Raghu, H. D. Revanasiddappa and B. Veeresh, *Cent. Nerv. Syst. Agents Med. Chem.*, 2015, **16**, 60-66.
30. Z. Sattar, M. R. Saberi and J. Chamani, *PLoS ONE*, 2014, **9**, e84045.
31. R. De-Llanos, S. Sánchez-Cortes, C. Domingo, J. V. García-Ramos and P. Sevilla, *J. Phys. Chem. C*, 2011, **115**, 12419-12429.
32. A. Tarushi, J. Kljun, I. Turel, A. A. Pantazaki, G. Psomas and D. P. Kessissoglou, *New J. Chem.*, 2013, **37**, 342-355.
33. H. G. O. Alvim, E. L. Fagg, A. L. de Oliveira, H. C. B. de Oliveira, S. M. Freitas, M.-A. E. Xavier, T. A. Soares, A. F. Gomes, F. C. Gozzo, W. A. Silva and B. A. D. Neto, *Org. Biomol. Chem.*, 2013, **11**, 4764-4777.
34. S. Datta, S. Panja and M. Halder, *J. Phys. Chem. B*, 2014, **118**, 12153-12167.
35. D. P. Yeggoni and R. Subramanyam, *Mol. BioSyst.*, 2014, **10**, 3101-3110.
36. A. Belatik, S. Hotchandani, J. Bariyanga and H. A. Tajmir-Riahi, *Eur. J. Med. Chem.*, 2012, **48**, 114-123.
37. D. C. Carter and J. X. Ho, *Adv. Protein Chem.*, 1994, **45**, 153-203.
38. G. Sudlow, D. J. Birkett and D. N. Wade, *Mol. Pharmacol.*, 1975, **11**, 824-832.
39. G. Sudlow, D. J. Birkett and D. N. Wade, *Mol. Pharmacol.*, 1976, **12**, 1052-1061.
40. E. Peyrin, Y. C. Guillaume and C. Guinchard, *Anal. Chem.*, 1998, **70**, 4235-4240.
41. H. A. Thörn, E. Sjögren, P. A. Dickinson and H. Lennernäs, *Mol. Pharmaceutics*, 2012, **9**, 3034-3045.
42. S. L. Zhuang, Z. S. Zhang, W. J. Zhang, L. L. Bao, C. Xu and H. Zhang, *Aquat. Toxicol.*, 2015, **159**, 119-126.
43. B. Ahmad, M. Z. Ahmed, S. K. Haq and R. H. Khan, *Biochim. Biophys. Acta – Proteins Proteomics*, 2005, **1750**, 93-102.
44. L. Galantini, C. Leggio and N. V. Pavel, *J. Phys. Chem. B*, 2008, **112**, 15460-15469.
45. E. Daniel and G. Weber, *Biochemistry*, 1966, **5**, 1893-1900.
46. A. Hawe, R. Poole and W. Jiskoot, *Anal. Biochem.*, 2010, **401**, 99-106.
47. M. Andujar-Sánchez, V. Jara-Perez, E. S. Cobos and A. Cámara-Artigas, *J. Mol. Recognit.*, 2011, **24**, 548-556.
48. I. M. Kuznetsova, A. I. Sulatskaya, O. I. Povarova and K. K. Turoverov, *PLoS ONE*, 2012, **7**, e40845.
49. L. Stryer, *J. Mol. Biol.*, 1965, **13**, 482-495.
50. L. Stryer, *Science*, 1968, **162**, 526-533.
51. G. M. Edelman and W. O. McClure, *Acc. Chem. Res.*, 1968, **1**, 65-70.
52. G. Sudlow, D. J. Birkett and D. N. Wade, *Mol. Pharmacol.*, 1973, **9**, 649-657.
53. L. A. Bagatolli, S. C. Kivatinitz, F. Aguilar, M. A. Soto, P. Sotomayor and G. D. Fidelio, *J. Fluoresc.*, 1996, **6**, 33-40.

54. A. E. A. Thumser, A. G. Buckland and D. C. Wilton, *J. Lipid Res.*, 1998, **39**, 1033-1038.
55. D. I. Cattoni, S. B. Kaufman and F. L. G. Flecha, *Biochim. Biophys. Acta – Proteins Proteomics*, 2009, **1794**, 1700-1708.
56. L. Stryer, *J. Biol. Chem.*, 2012, **287**, 15164-15173.
57. D. C. Carter, in *Burger's Medicinal Chemistry and Drug Discovery*, ed. D. J. Abraham and D. P. Rotella, John Wiley & Sons, Inc., Hoboken, NJ, 7th edn., 2010, pp 437-467.
58. T. Peters Jr., in *All about Albumin: Biochemistry, Genetics, and Medical Applications*, Academic Press, San Diego, CA, 1995, pp 9-132.
59. M. T. Montero, R. Pouplana, S. García and O. Valls, *J. Pharm. Pharmacol.*, 1986, **38**, 925-927.
60. U. Kragh-Hansen, *Mol. Pharmacol.*, 1988, **34**, 160-171.
61. T. C. Pinkerton and K. A. Koeplinger, *Anal. Chem.*, 1990, **62**, 2114-2122.
62. N. P. Sollenne and G. E. Means, *Mol. Pharmacol.*, 1979, **15**, 754-757.
63. U. Kragh-Hansen, *Biochem. J.*, 1985, **225**, 629-638.
64. R. Brodersen, T. Sjödin and I. Sjöholm, *J. Biol. Chem.*, 1977, **252**, 5067-5072.
65. J.-P. Tillement, R. Zini, M. Lecomte and P. d'Athis, *Eur. J. Drug Metab. Pharmacokinet.*, 1980, **5**, 129-134.
66. J. A. Hamilton, *Biochim. Biophys. Acta – Gen. Subj.*, 2013, **1830**, 5418-5426.
67. B. A. Bondesen and M. D. Schuh, *J. Chem. Educ.*, 2001, **78**, 1244-1247.
68. L. A. Abriata, *J. Chem. Educ.*, 2011, **88**, 1268-1273.
69. N. J. Greenfield, *Nat. Protoc.*, 2006, **1**, 2876-2890.
70. G. Pescitelli, L. Di Bari and N. Berova, *Chem. Soc. Rev.*, 2014, **43**, 5211-5233.
71. D. Leckband and J. Israelachvili, *Q. Rev. Biophys.*, 2001, **34**, 105-267.
72. M. T. Record Jr., C. F. Anderson and T. M. Lohman, *Q. Rev. Biophys.*, 1978, **11**, 103-178.
73. J. D. Chodera and D. L. Mobley, *Annu. Rev. Biophys.*, 2013, **42**, 121-142.
74. P. D. Ross and S. Subramanian, *Biophys. J.*, 1980, **32**, 79-81.
75. P. D. Ross and S. Subramanian, *Biochemistry*, 1981, **20**, 3096-3102.
76. J. E. Jones, *Proc. R. Soc. A: Math., Phys. Eng. Sci.*, 1924, **106**, 441-462.
77. T. M. C. Faro, G. P. Thim and M. S. Skaf, *J. Chem. Phys.*, 2010, **132**, 114509.